Below-threshold harmonic generation in gas-jets for Th-229 nuclear spectroscopy

ARTHUR SCHÖNBERG,[1] SARPER SALMAN,[1,2,3] AYHAN TAJALLI,[1] SONU KUMAR,[1] INGMAR HARTL[1] AND CHRISTOPH M. HEYL[1,2,3]

[1]*Deutsches Elektronen-Synchrotron DESY, Notkestr. 85, 22607 Hamburg, Germany*
[2]*Helmholtz-Institute Jena, Fröbelstieg 3, 07743 Jena, Germany*
[3]*GSI Helmholtzzentrum für Schwerionenforschung GmbH, Planckstraße 1, 64291 Darmstadt, Germany*
**arthur.schoenberg@desy.de*

Abstract: The generation of below-threshold harmonics in gas-jets constitutes a promising path towards optical frequency combs in the vacuum ultra-violet (VUV) spectral range. Of particular interest is the 150 nm range, which can be exploited to probe the nuclear isomeric transition of the Thorium-229 isotope. Using widely available high-power, high-repetition-rate Ytterbium-based laser sources, VUV frequency combs can be generated through the process of below-threshold harmonic generation, in particular 7th harmonic generation of 1030 nm. Knowledge about the achievable efficiencies of the harmonic generation process is crucial for the development of suitable VUV sources. In this work, we measure the total output pulse energies and conversion efficiencies of below-threshold harmonics in gas-jets in a phase-mismatched generation scheme using Argon and Krypton as nonlinear media. Using a 220 fs, 1030 nm source, we reach a maximum conversion efficiency of 0.72×10^{-5} for the 7th harmonic (147 nm) and 0.7×10^{-4} for the 5th harmonic (206 nm). In addition, we characterize the 3rd harmonic of a 178 fs, 515 nm source with a maximum efficiency of 0.29%.

1. Introduction

Harmonic generation in crystals, along with the mixing of light of different frequencies through parametric processes, results in a continuum of accessible laser wavelengths ranging from vacuum-ultraviolet (VUV) [1] over the optical and near-infrared (NIR) [2], down to mid-infrared (MIR) [3] and even the terahertz (THz) regime [4]. On the other hand, high-harmonic generation (HHG) in gases provides the possibility to produce coherent light ranging from extreme-ultraviolet (XUV) up to the soft X-ray regime [5,6]. In-between these spectral regions, a less-explored wavelength regime can be identified, roughly located between the cut-off wavelength of the $KBeBO_3F_2$ (KBBF) crystal (about 150 nm) and the wavelength regime defined e.g. by the ionization threshold of e.g. Xenon (about 100 nm). The harmonics produced in this regime are often referred to as below-threshold harmonics (BTH). The BTH regime is increasingly gaining attention, brought along by the recent progress in nuclear spectroscopy research [7,8]. In particular, a very special nuclear state of the Thorium-229 isotope, the ^{229m}Th nuclear isomeric state, is characterized by an exceptionally low transition energy [8–10]. While most of the known nuclear transition energies in atomic nuclei are located in energy ranges far above the photon energies of conventional laser sources, recent measurements of the ^{229m}Th isomeric state revealed that the energy of this transition lies within the 1σ-interval of 7.88 eV < E < 8.16 eV, corresponding to a wavelength interval of 157.34 nm > λ > 151.94 nm in the VUV-range[7] In a more recent experiment a transition energy of 8.338 eV ± 0.024 eV was measured, corresponding to a wavelength of 148.71 nm ± 0.42 nm [8]. Another remarkable property of the nuclear isomeric state ^{229m}Th is its long lifetime of the order of 10^3-10^4 seconds [12,13] for charged Thorium-229 in the so-called radiative decay channel. This corresponds to a very narrow transition linewidth in the mHz range or lower [14]. A kHz level line is expected for the so-called internal conversion decay channel occurring in neutral Thorium-229. In order

to excite this transition directly, laser light can prospectively be used, requiring a suitable wavelength range, as well as an extremely narrow line-width [14]. A promising laser source is an optical frequency-comb (OFC) [13,14], which consist of many equally spaced narrow-line-width comb-teeth with a spacing defined by the pulse repetition rate f_{rep} of the laser [16]. Using Ytterbium-based OFCs at 1030 nm wavelength, the most straightforward approach for obtaining an OFC with the required wavelength around 150 nm is 7th harmonic generation in gases. Such an OFC can prospectively be used to directly probe the nuclear transition of Thorium-229 and immensely narrow down the uncertainties regarding the exact energy of this transition [7]. Thus, the development of a suitable 150 nm OFC source via harmonic generation in gases requires thorough knowledge of the BTH generation process.

BTH generation has been studied in multiple works [17]. Of particular interest has been the question whether the BTH generation process can be described within a perturbative framework, or whether strong-field quantum effects such as quantum electron-path interferences and effects from the ion-core potential play a role in the generation process [18]. Also, the generation of BTH of an OFC within a passive enhancement cavity has been studied [17,18] as well as the coherence properties of such intra-cavity generated extreme-UV comb [21]. However, a detailed study on the harmonic generation conversion efficiencies in the BTH regime in gases, along with an analysis of the macroscopic generation conditions has not been reported.

In this work we address this issue and measure the total output pulse energy and efficiency of the 7th harmonic of a 1030 nm laser source in rare gases, resulting in a wavelength of about 147 nm. In addition, we perform similar measurements for the 5th harmonic of the 1030 nm source (206 nm) and explore a cascaded harmonic generation scheme, where we generate the 6th harmonic (172 nm) of the 1030 nm source via the 3rd harmonic of the 2nd harmonic (515 nm). The measurements are performed in a phase-mismatched generation scheme arising due to non-favorable dispersion characteristics in the VUV, which limits the harmonic yield. Based on the results of this work, we further provide estimates considering intra-cavity 7th harmonic generation, revealing a sufficiently high frequency conversion efficiency to match the requirements estimated e.g. for driving nuclear Rabi transitions in a single Thorium-229 ion.

This paper is organized as follows: in section 2 we introduce and compare different schemes for VUV-light generation, which may be suitable for nuclear spectroscopy of Thorium-229. In section 3 the experimental setup and methods are shown. In section 4 we present experimental results on the conversion efficiencies and output pulse energies for 3rd, 5th, and 7th harmonic generation in Argon and Krypton. We discuss the results in the context of a potential experimental setup for Thorium-229 nuclear spectroscopy. In section 5 we conclude our findings.

2. VUV frequency conversion schemes

The production of temporally coherent light at 150 nm in the VUV spectral range is not limited to direct 7th harmonic generation of 1030 nm laser sources in gas-jets. In this section we briefly discuss different methods available. The main focus lies on the practicability of these methods for producing a suitable source in order to probe the nuclear isomer transition of Thorium-229.

2.1 VUV generation in nonlinear crystals

Harmonic generation in nonlinear crystals is a highly developed field and widely used as a frequency conversion technique. Yet the majority of commonly used nonlinear crystals become absorptive in the VUV range below a certain wavelength [20,21]. At the same time, the efficiency of harmonic generation in crystals can greatly profit from a high nonlinearity as well

as the non-isotropy of crystals, providing the possibility of achieving phase-matching via dispersion tuning e.g. by angle adjustment of the crystal.

A promising crystal for frequency conversion below 150 nm is KBBF [22-24]. The wavelength-dependent absorption in KBBF shows a cutoff wavelength of 147 nm, down to which it still remains transparent [25]. It has been demonstrated that wavelengths down to 149.8 nm can be produced via sum-frequency generation in a KBBF crystal [1]. There, the fundamental beam with a tunable wavelength range of 749-790 nm and its 4th harmonic at around 187-198 nm was used to generate the 5th harmonic via sum-frequency generation in a phase-matched manner. Relative to the 4th harmonic input of 170 mW, the efficiency of the 5th harmonic amounted to 2.3×10^{-5} for 149.8 nm and reached up to 4×10^{-4} for 158 nm. In this experiment, pulses of 1.6 ns with a comparatively narrow spectral bandwidth of 1.4 GHz were used as the fundamental beam. The 4th harmonic pulse duration was 0.4 ns, resulting in a pulse duration of 0.4 ns of the 5th harmonic [1]. It is yet to be shown that more efficient generation of VUV-femtosecond pulses is possible within a KBBF crystal.

2.2 VUV generation in hollow-core fibers

Gas-filled hollow-core fibers (HCF) offer a range of possibilities for nonlinear frequency conversion. They can be used for spectral broadening and pulse compression [27,28], white-light generation [29], as well as cascaded frequency mixing [30]. Most notably, gas-filled HCFs provide the possibility to generate VUV radiation efficiently. Travers and co-workers showed that tunable ultrashort VUV-pulse can be generated in HCFs via the resonant-dispersive-wave (RDW) mechanism [31]. Using Helium-filled fibers with large core sizes of 75-500 µm, ultrashort high-energy pulses of up to a few mJ can be coupled into a HCF. The subsequent formation of solitons and their dispersion dynamics lead to the resonant generation of broadband tunable emission, when linear- and nonlinear dispersion effects balance out [31]. Through the process of RDW-emission, efficiencies of up to 1.8 % have been reached for 147 nm generation with a pump wavelength of 800 nm and for 157 nm the efficiency went up to as high as 3.2 % [31].

As another approach to VUV generation in gas-filled HCFs, a highly cascaded harmonic generation scheme has been put forward. Relying on a four-wave mixing (FWM) process, this method can produce phase-matched cascaded harmonics starting from the 3rd harmonic of a 1035 nm source up to the 9th and each harmonic in between [30]. For the 7th harmonic, efficiencies up to 1.2×10^{-5} were achieved [30].

Instead of using simple, gas-filled hollow capillaries, one can exploit the benefits of structured photonic-crystal HCF. In particular, gas-filled kagomé-type HCFs exhibit wide dispersion tunability and thus enable flexible tuning of phase-matching e.g. in an FWM scheme [32]. Deep-UV pulses at 266 nm have been generated using such a scheme employing low pump pulse energies in the range of 1 µJ with conversion efficiencies of up to 38% [33], with prospects to reach even shorter wavelengths down to the VUV by choosing the correct pump and seed wavelengths, as well as pressure [33]. This method could enable high-repetition rate, high-power IR sources to be converted into the VUV in a highly efficient manner. However, it remains to be shown that the HCF-based conversion of IR pulses into the VUV preserves the coherence of the driving OFC. Regarding a possible application for nuclear spectroscopy of Thorium-229, transfer of coherence from the source to the converted light is a crucial requirement.

2.3 VUV-generation in gases

A more straightforward approach to generating coherent VUV light is the direct generation of below-threshold harmonics in gases. Below-threshold harmonics, such as high-order harmonics, can be generated by directly focusing intense ultrashort infrared pulses into a gas target [18].
The generation of harmonics in gas-jets can additionally be incorporated into a passive enhancement cavity [7,19,20,34–36]. When the carrier-envelope-phase and the repetition rate of a laser source are stabilized, pulses can be coherently superimposed inside a repetition-rate-matched and -locked enhancement cavity [37]. This is particularly suitable for high repetition rate sources, where the pulse energy is rather low, e.g. in the µJ level. With such a source, intra-cavity pulse energies can be enhanced by a factor of more than 100 [20], supporting sufficiently high intensities for generating below-threshold and high-order harmonics in a gas-jet at high repetition rates demanded for frequency combs reaching beyond 10 or even 100 MHz. Out-coupling of the generated harmonics can be achieved efficiently with up to 70% demonstrated out-coupling-efficiency [7].
An important advantage of gas harmonics is the transfer of coherence from the source to the harmonic. It has been shown that the harmonic generation process in gas-jets supports coherence times beyond 1 s [21] thus providing promising characteristics for Th-229 spectroscopy [12]. However, the direct generation of the 7^{th} harmonic of 1030 nm, as well as below-threshold harmonics in general, is expected to lead to comparatively low efficiencies and output pulse energies due to an inevitably phase-mismatched generation process. For high-harmonic generation in gases, contributions to phase matching between fundamental and harmonic light field typically have opposite signs and thus phase-matching is achieved e.g. by tuning the gas pressure [38,39]. In contrast, this approach is not feasible for BTH generation of 1030 nm in most gases as the dispersion contributions stemming from the neutral gas and the generated plasma have the same sign, causing a phase-mismatch which limits the efficiency of this process. In the following sections, we show that despite these limitations, sufficiently efficient below-threshold harmonics can be generated in gas-jets using Argon and Krypton.

3. Experimental setup and methods

In this section we introduce the experimental setup as well as the methods we use in order to obtain the pulse energies and conversion efficiencies of the measured harmonics.

3.1 Experimental setup

Our setup mainly consists of the following components: a laser system, an attenuation unit, a vacuum system, a nozzle and gas supply, and a detector, as shown in Fig. 1. The laser system is a commercially available Yb:YLF based laser (PHAROS) with a center-wavelength of 1030 nm. It delivers pulses up to 200 µJ with a repetition rate of up to 100 kHz thus resulting in an average power of 20 W and pulse durations of around 220 fs, which we measured via autocorrelation and frequency-resolved optical gating (FROG) techniques. The laser is equipped with an internal pulse-picking option, which we use to decrease the pulse repetition rate down to 10-20 kHz. Following the laser output, the beam is guided into the attenuation unit, consisting of a λ/2 waveplate and a thin-film polarizer (TFP). The transmitted p-polarized beam is coupled into the vacuum chamber through an anti-reflection (AR) coated window. Inside the vacuum chamber the beam is focused onto the target medium – the gas-jet – by a simple spherical lens of 100 mm or 150 mm focal length. Subsequently after generating harmonics inside the gas-jet, the beams are separated by a CaF_2 prism. After separation the fundamental beam is guided out of the chamber onto a beam dump. The generated VUV-beams

transmitted through the CaF_2 prism are detected by a fluorescent plate and the target beam e.g. the 7th harmonic is guided onto and detected by a UV-photo diode.

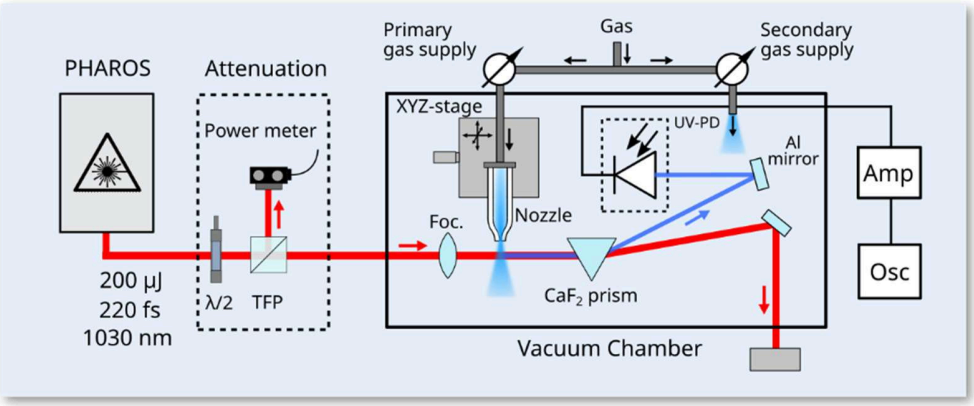

Fig. 1. Experimental setup used for generation and detection of below-threshold gas harmonics. As a source a commercial 1030 nm laser system with 200 µJ pulse energy and 220 fs pulse duration is used. The light is attenuated by a waveplate and a thin-film polarizer (TFP). The gas target is generated by a glass nozzle, positioned with an xyz stage. After harmonic generation the light is separated by a CaF_2 prism, where the harmonic is aligned onto a UV-photodiode (UV-PD). The signal is read out by a current amplifier (Amp) and an oscilloscope (Osc).

For pressure-controlled gas supply we use a pressure reducer with a continuously tunable pressure range of 0-18 bar. Besides pulse energy control, the pressure tunability provides control of the other key parameter for the experiment, the particle density of the harmonic generation medium. We use custom-built nozzles with orifice diameters of 50 µm, 100 µm, and 200 µm and a very short converging section at the nozzle tip to minimize gas flow limitations. Another key element is the secondary gas supply, which is used to tune the ambient pressure in the chamber. Ambient pressure tuning provides a way to measure the re-absorption of the generated harmonic signal in the gas.
Detection of the VUV harmonics is achieved by a silicon-based calibrated UV photo diode (Opto Diode AXUV576C UV) (UV-PD) with an area of 24 mm×24 mm. The responsivity of the diode according to the specifications amounts to 0.12 A/W for 147 nm light. The signal of the diode is measured by applying a bias voltage of 4 V and using a SRS570 low-noise current amplifier. In order to reduce stray light and noise on the diode, an appropriate shielding is applied. The calibration of the photodiode and the calculation of the pulse energies from the recorded oscilloscope traces was verified for 1030 nm [40], using the same type of photodiode and the PHAROS laser system we use in our experiment.

3.2 Experimental methods

For VUV characterization, we use a similar detection scheme as used in Ref. [40]. The background-corrected signal trace $S(t)$ is converted into a pulse energy via [40]

$$E_{\mathrm{UV}} = \frac{1}{n_{\mathrm{p}}} \frac{\mathrm{G}}{\mathrm{R}} \int S(t)\, dt\,, \quad (1)$$

where n_p is the number of pulses in the signal trace, G is the sensitivity (Gain) of the current amplifier in units of A/V and R is the responsivity of the UV-PD. The integration is carried out over the whole time window of the signal trace. In order to obtain correct results for the conversion efficiencies reached in the gas jet, losses due to re-absorption of the harmonic signal inside the residual gas must be considered.

The amount of re-absorbed light depends on the wavelength, gas type, ambient pressure of the residual gas and the propagation length. We measure the re-absorption of 7th, 6th, and 5th harmonic corresponding to wavelengths of about 147 nm, 172 nm and 206 nm in the corresponding gases, in which the harmonics are generated. It is important to note that re-absorption, especially in the VUV range, strongly depends on the purity of the gas [41]. The process of absorption of light in a medium after propagating a distance z can be modeled by the simple exponential law $\mathrm{I}(\mathrm{p}, z) = \mathrm{I}(0,0)\exp(-\kappa \mathrm{pz})$ [42], where I is the intensity, p the pressure, z the propagation length and κ the absorption coefficient we want to measure. Measurements of the absorption coefficients require control over either the propagation length, or the pressure of the medium. By measurement of the harmonic signals at different pressure levels, the wavelength and gas-type dependent coefficient κ can be extracted via linear regression on semi-logarithmic plot of the measured signal strengths, enabling us to estimate the signal strength before propagation through the residual gas medium.

Re-absorption naturally occurs during the harmonic generation process within the generation medium – i.e. the gas jet – itself. The gas jet density, however, is expected to vary only little when the ambient chamber pressure is changed. Consequently, our re-absorption measurements do not take re-absorption inside the gas jet into account. Considering that upon installation of suitable differential pumping units, re-absorption behind the gas jet can be avoided, we are mainly interested in the possible harmonic yield directly after harmonic generation medium.

In addition to re-absorption in the residual ambient gas, we must also consider the losses which occur due to the CaF_2 prism used to separate the harmonics. The prism surface is uncoated and thus reflection losses on the surfaces can be simply calculated using Snell's law. Absorption of the harmonics within the CaF_2 prism are accounted for using reported transmission data for CaF_2 [43].

4. Results

In this chapter, we present the results of 7th harmonic, as well as 5th harmonic and cascaded 6th harmonic generation measurements.

4.1 7th harmonic of 1030 nm

The conversion efficiency of a 7th harmonic generation process in gas jets depends on the pressure of the gas applied on the nozzle — or more precisely the particle density — as well as the pulse energy and the focal geometry of the fundamental beam. In our experiment, we choose two gases as nonlinear media, Argon and Krypton at a fixed focal geometry. The beam is focused down with a lens of 100 mm focal length, resulting in an estimated maximum peak Intensity of around 2×10^{14} W/cm^2 (if beam-distorting effects such as plasma defocusing are neglected). Another important parameter is the length of the medium, which is determined by the nozzle orifice diameter. In this experiment we use two different nozzles with 50 µm and 100 µm diameter.

Figure 2 shows the 7th harmonic generation results for a 100 µm nozzle in Argon and Krypton. The plots depict the measured output pulse energies and efficiencies as a function of laser input pulse energy and backing gas pressure applied on the nozzle. In both cases the measurements were conducted under similar experimental conditions and only the gas was exchanged.

In case of Argon (Figs. 2a and 2b), the maximum 7th harmonic pulse energy reaches 0.65 nJ at the highest laser pulse energy and gas pressure. The output VUV pulse energy is not fully saturated and exhibits an increasing trend at maximum input parameters. On the other hand, the efficiency (Fig. 2b) reaches a maximum of 0.37×10^{-5} at an input of about 150 µJ laser pulse energy.

In Krypton we observe an efficiency maximum at lower input energies at around 110 µJ, reaching up to 0.65×10^{-5} and a maximum output pulse energy of about 0.81 nJ as shown in Fig. 2. Corresponding results for the 50 µm nozzle in Krypton are displayed in Fig. 3, where the efficiency reaches 0.72×10^{-5} and the output pulse energy 1 nJ.

While the maximum UV pulse energy in Krypton is only slightly higher than in Argon, the maximum efficiency is roughly twice as high. Since it appears that the VUV output energy is still not in full saturation in the case of Argon (Fig. 2a), the maximum pulse energy output could potentially reach a similar value as the one in Krypton. On the other hand, the maximum conversion efficiency already reaches its peak and would only decrease with higher input IR energies.

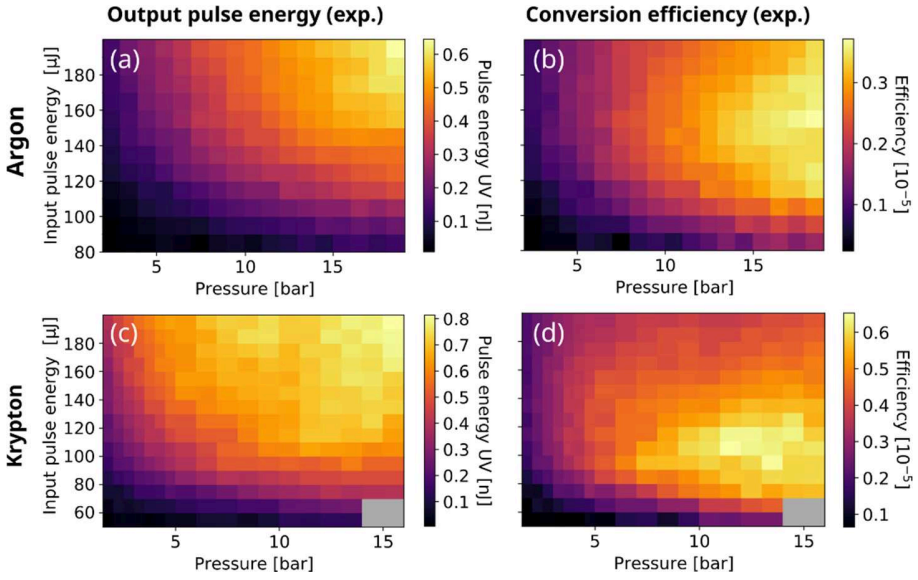

Fig. 2. Results for the 7th harmonic output pulse energy (a, c) and conversion efficiency (b, d) in Argon (a,b) and Krypton (c,d) with a 100 µm nozzle orifice diameter. The measurements are taken as a function of pressure and input pulse energy of the fundamental 1030 nm source. Missing datapoints are indicated in grey.

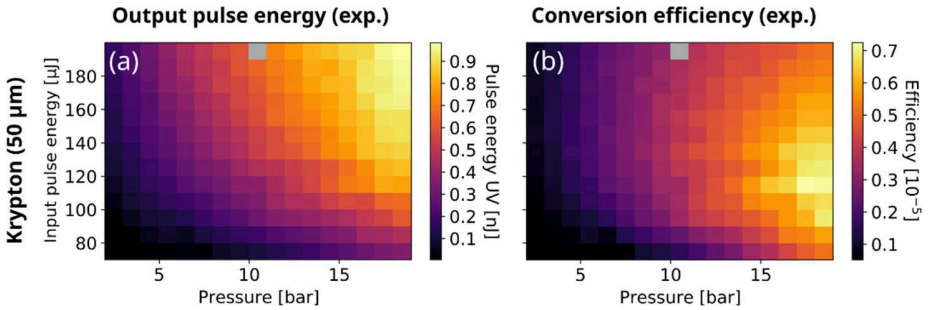

Fig. 3. Results for the 7th harmonic output pulse energy and conversion efficiency in Krypton for a smaller nozzle of 50 µm diameter. (a) shows the experimental data for the output 7th harmonic pulse energy and (b) the efficiency derived from the output pulse energy. Missing datapoints are indicated in grey.

Harmonic generation in both Argon and Krypton exhibit a similar behavior in terms of harmonic efficiency as a function of input pulse energy (intensity) and gas pressure. At lower intensities we observe an increase in efficiency, which saturates at a certain intensity and decreases at higher intensities. Similarly, when tuning the pressure (particle density) from lower to higher values, we first observe an increase in harmonic efficiency until the signal saturates.

These general trends for pulse energy and harmonic efficiency showing an increasing signal with laser intensity and gas pressure reflect very well the behavior expected for harmonic generation in gases. While the single-atom harmonic yield increases with intensity, the number of emitters grows with gas pressure, thus resulting in an increasing harmonic signal emitted. For HHG in gases where phase-matched generation is possible, this signal increase is further affected by phase-matching conditions which improve until an intensity-dependent phase matching pressure is reached [38,39]. In contrast, for BTH in gases, phase-matching is constantly deteriorating with increasing intensity and pressure. However, our results indicate that the nonlinear signal growth can easily dominate the negative effect of an increasing phase-mismatch in the low pressure/intensity regime. A signal maximum can likely be attributed to multiple effects such as signal depletion at high intensity when a large ionization fraction is reached, plasma defocusing as well as to limitations of the macroscopic signal buildup arising due to re-absorption of the generated harmonics at high gas density.

4.2 5th harmonic and cascaded 6th harmonic of 1030 nm

Following our 7th harmonic generation experiments we additionally measure the 5th harmonic and cascaded 6th harmonic output pulse energies and conversion efficiencies. In order to generate the 6th harmonic, we use the 2nd harmonic output of the PHAROS laser system at 515 nm and generate the 3rd harmonic in Argon. In both cases we use a nozzle of 200 µm orifice diameter.
In Fig. 4 the measured data is shown for the 5th harmonic. Again, the 5th harmonic pulse energy (Fig. 4a) and efficiency (Fig. 4b) are plotted as a function of nozzle backing pressure and input IR pulse energy. The experimental conditions are similar to the 7th harmonic experiments, only the nozzle orifice diameter is changed to 200 µm. For the 5th harmonic of 1030 nm we measure a maximum pulse energy of 8 nJ and a maximum conversion efficiency of 0.7×10^{-4}. Similar to the 7th harmonic, the efficiency maximum appears at an input pulse energy of 100-110 µJ.

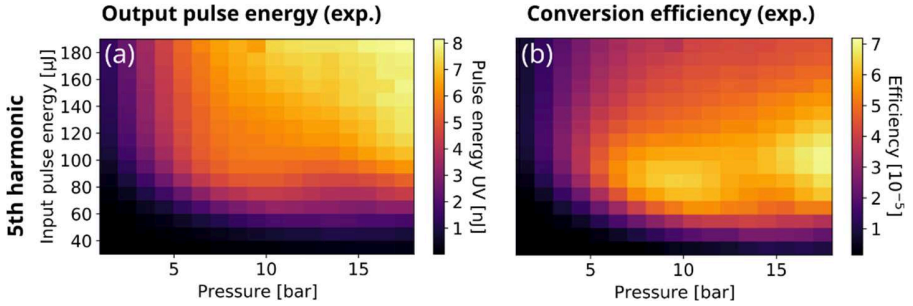

Fig. 4. Experimental results for the 5th harmonic (206 nm) output pulse energy (a) and corresponding conversion efficiency (b) in Krypton for a nozzle with 200 µm orifice diameter.

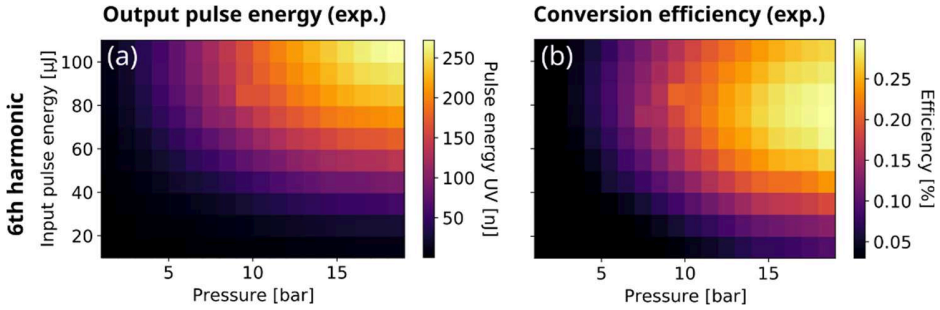

Fig. 5. Experimental results for the cascaded 6th harmonic (172 nm) output pulse energy (a) and corresponding conversion efficiency (b) in Argon for a nozzle with 200 µm orifice diameter.

In addition, we observe a second peak in efficiency at lower pressures at roughly 10 bar and slightly lower input energy (Fig. 4b).

In the cascaded 6th harmonic experiment we chose Argon as the nonlinear medium and a nozzle orifice diameter of 200 µm. The results are displayed in Figure 5. Here, the second harmonic output of the laser centered at 515 nm is guided onto the target with a maximum pulse energy of 100 µJ at the target. We measure a pulse length of 178 fs at the output of the laser. In this setup we chose a looser focal geometry of 150 mm focal length. Considering the given beam parameters from the laser system we calculate a peak intensity up to 1.3×10^{14} W/cm^2 in the focus in vacuum.
Here we measure a maximum of 270 nJ output pulse energy and a maximum efficiency of 0.29%. The efficiency is directly calculated in relation to the 2nd harmonic input pulse energy. Considering 2nd harmonic conversion efficiencies of 1030 nm sources reaching up to 70% [44], a total cascaded 6th harmonic efficiency of about 0.2% can be considered realistic.

The general behavior of 5th and 6th harmonic signal with increasing intensity and pressure reflects similar trends as observed for the 7th harmonic. In the 5th harmonic (Fig. 4) however, we observe a double efficiency maximum with increasing gas pressure. Effects like pressure-dependent phase-matching and/or nonlinear laser pulse reshaping at high pressures can lead to multi-peak structures for HHG as reported in earlier works [45]. A detailed analysis of this effects for BTH goes beyond the scope of this work.

In a perturbative picture, the generation of 7th, 5th and cascaded 6th harmonic are processes that depend on the nonlinear 7th, 5th and 3rd order responses of the medium, respectively. Hence, we

expect a strong increase in signal strength when reducing the nonlinear order. This is reflected by our measurements: the output pulse energies increase by an order of magnitude from the 7th to 5th and from the 5th to the 3rd harmonic of the 2nd harmonic. The same conclusion can be drawn for the efficiency. We see an increase of more than an order of magnitude for each step down in the harmonic order.

4.3 Discussion of results regarding a 150 nm OFC for nuclear spectroscopy of Thorium-229

In view of the requirements for nuclear spectroscopy of Thorium-229, we can follow Ref. [7] and estimate if the measured 7th harmonic efficiency can be deemed sufficient to build a laser for driving the given nuclear isomeric transition. We base our estimates on demonstrated approaches for VUV comb production considering intra-cavity harmonic generation. Assuming an OFC source at 1030 nm central wavelength, 200 fs pulse duration, 65 MHz repetition rate, a laser average power of 84 W, as reported e.g. in Ref. [46], and a passive enhancement cavity with a realistic enhancement factor of 100 [18], an intra-cavity peak intensity $> 1\times10^{14}$ W/cm^2 can be reached. Taking into account our measurements of the conversion efficiency of 7th harmonic generation reaching a maximum of 0.72×10^{-5}, we can conservatively assume an efficiency of 0.2×10^{-5}, considering a reduced efficiency due to intra-cavity intensity clamping, which typically limits the intensity which can be reached inside an intra-cavity gas jet compared to single-pass experiments. Using these parameters while taking into account a bandwidth of the generated 7th harmonic of 100 meV and further assuming beam transport losses of 75% including out-coupling losses [47], we end up with an available power per comb tooth of about 10 nW, which is equivalent to the power considered in Ref. [7], providing multiple options for direct laser-driven Th-229 spectroscopy. Consequently, we can conclude that the requirements specified in Ref. [7] for driving the nuclear transition of a single Th-229 ion with a 150 nm VUV-frequency comb can be fulfilled. Furthermore, we demonstrated that by exploiting lower-order harmonic generation, such as the 5th or 3rd harmonic, the conversion efficiency can be greatly enhanced, opening opportunities for alternative frequency conversion routes for efficient 150 nm production.

5. Conclusion

In this work we study below-threshold harmonic generation in Argon and Krypton using 1030 nm pulses as the fundamental wavelength. We measure the output pulse energies as well as conversion efficiencies of the 7th (147 nm), 5th (206 nm), as well as the 3rd harmonic of the 2nd harmonic (172 nm). We show that within the parameter range of our measurements, we can reach conversion efficiencies up to 0.7×10^{-5} for the 7th harmonic in Krypton. We estimate that this value is sufficient for nuclear spectroscopy experiments of charged Thorium-229. Furthermore, we confirm that lower order harmonic generation in gases, such as the 3rd or 5th harmonic, results in orders-of-magnitude higher conversion efficiencies. The phase-mismatched generation conditions are identified as the main limiting factor for efficient generation of BTH in the here discussed wavelength regime.

References

1. T. Nakazato, I. Ito, Y. Kobayashi, X. Wang, C. Chen, and S. Watanabe, "Phase-matched frequency conversion below 150 nm in $KBe_2BO_3F_2$," Opt. Express **24**(15), 17149 (2016).
2. B. J. Cole, S. Chinn, and L. Goldberg, "Near-IR, blue, and UV generation by frequency conversion of a Tm:YAP laser," in *Solid State Lasers XXVII: Technology and Devices*, W. A. Clarkson and R. K. Shori, eds. (SPIE, 2018).
3. B.-H. Chen, T. Nagy, and P. Baum, "Efficient middle-infrared generation in $LiGaS_2$ by simultaneous spectral broadening and difference-frequency generation," Opt. Lett. **43**(8), 1742 (2018).
4. H. T. Olgun, W. Tian, G. Cirmi, K. Ravi, C. Rentschler, H. Çankaya, M. Pergament, M. Hemmer, Y. Hua, D. N. Schimpf, N. H. Matlis, and F. X. Kärtner, "Highly efficient generation of narrowband terahertz radiation driven by a two-spectral-line laser in PPLN," Opt. Lett. **47**(10), 2374 (2022).
5. A. McPherson, G. Gibson, H. Jara, U. Johann, T. S. Luk, I. A. McIntyre, K. Boyer, and C. K. Rhodes, "Studies of multiphoton production of vacuum-ultraviolet radiation in the rare gases," J. Opt. Soc. Am. B **4**(4), 595 (1987).
6. M. Ferray, A. L'Huillier, X. F. Li, L. A. Lompre, G. Mainfray, and C. Manus, "Multiple-harmonic conversion of 1064 nm radiation in rare gases," J. Phys. B At. Mol. Opt. Phys. **21**(3), L31–L35 (1988).
7. L. von der Wense and C. Zhang, "Concepts for direct frequency-comb spectroscopy of ^{229m}Th and an internal-conversion-based solid-state nuclear clock," Eur. Phys. J. D **74**(7), (2020).
8. S. Kraemer, J. Moens, M. Athanasakis-Kaklamanakis, S. Bara, K. Beeks, P. Chhetri, K. Chrysalidis, A. Claessens, T. E. Cocolios, J. M. Correia, H. De Witte, R. Ferrer, S. Geldhof, R. Heinke, M. Hosseini, R. Lica, G. Magchiels, V. Manea, C. Merckling, L. M. C. Pereira, S. Raeder, T. Schumm, S. Sels, P. G. Thirolf, S. M. Tunhuma, P. Van Den Bergh, P. Van Duppen, A. Vantomme, M. Verlinde, R. Villarreal, and U. Wahl, "Observation of the radiative decay of the ˝229\backslashmathrm Th nuclear clock isomer," arXiv:2209.10276 (2022).
9. B. R. Beck, J. A. Becker, P. Beiersdorfer, G. V. Brown, K. J. Moody, J. B. Wilhelmy, F. S. Porter, C. A. Kilbourne, and R. L. Kelley, "Energy Splitting of the Ground-State Doublet in the Nucleus ^{229}Th," Phys. Rev. Lett. **98**(14), (2007).
10. A. Yamaguchi, H. Muramatsu, T. Hayashi, N. Yuasa, K. Nakamura, M. Takimoto, H. Haba, K. Konashi, M. Watanabe, H. Kikunaga, K. Maehata, N. Yamasaki, and K. Mitsuda, "Energy of the ^{229}Th Nuclear Clock Isomer Determined by Absolute γ-ray Energy Difference," Phys. Rev. Lett. **123**(22), (2019).
11. B. Seiferle, L. von der Wense, P. V. Bilous, I. Amersdorffer, C. Lemell, F. Libisch, S. Stellmer, T. Schumm, C. E. Düllmann, A. Pálffy, and P. G. Thirolf, "Energy of the ^{229}Th nuclear clock transition," Nature **573**(7773), 243–246 (2019).
12. E. V. Tkalya, C. Schneider, J. Jeet, and E. R. Hudson, "Radiative lifetime and energy of the low-energy isomeric level in ^{229}Th," Phys. Rev. C **92**(5), (2015).
13. B. Seiferle, L. von der Wense, and P. G. Thirolf, "Lifetime Measurement of the ^{229}Th nuclear isomer," Phys. Rev. Lett. **118**(4), (2017).
14. L. von der Wense, P. V. Bilous, B. Seiferle, S. Stellmer, J. Weitenberg, P. G. Thirolf, A. Pálffy, and G. Kazakov, "The theory of direct laser excitation of nuclear transitions," Eur. Phys. J. A **56**(7), (2020).
15. T. Udem, J. Reichert, R. Holzwarth, and T. W. Hänsch, "Accurate measurement of large optical frequency differences with a mode-locked laser," Opt. Lett. **24**(13), 881 (1999).
16. T. Fortier and E. Baumann, "20 years of developments in optical frequency comb technology and applications," Commun. Phys. **2**(1), (2019).
17. W.-H. Xiong, L.-Y. Peng, and Q. Gong, "Recent progress of below-threshold harmonic generation," J. Phys. B At. Mol. Opt. Phys. **50**(3), 032001 (2017).
18. D. C. Yost, T. R. Schibli, J. Ye, J. L. Tate, J. Hostetter, M. B. Gaarde, and K. J. Schafer, "Vacuum-ultraviolet frequency combs from below-threshold harmonics," Nat. Phys. **5**(11), 815–820 (2009).
19. A. K. Mills, T. J. Hammond, M. H. C. Lam, and D. J. Jones, "XUV frequency combs via femtosecond enhancement cavities," J. Phys. B At. Mol. Opt. Phys. **45**(14), 142001 (2012).
20. A. Cingöz, D. C. Yost, T. K. Allison, A. Ruehl, M. E. Fermann, I. Hartl, and J. Ye, "Direct frequency comb spectroscopy in the extreme ultraviolet," Nature **482**(7383), 68–71 (2012).
21. C. Benko, T. K. Allison, A. Cingöz, L. Hua, F. Labaye, D. C. Yost, and J. Ye, "Extreme ultraviolet radiation with coherence time greater than 1 s," Nat. Photonics **8**(7), 530–536 (2014).
22. D. Eimerl, L. Davis, S. Velsko, E. K. Graham, and A. Zalkin, "Optical, mechanical, and thermal properties of barium borate," J. Appl. Phys. **62**(5), 1968–1983 (1987).
23. D. N. Nikogosyan, "Lithium triborate (LBO)," Appl. Phys. Solids Surf. **58**(3), 181–190 (1994).
24. T. Kanai, T. Kanda, T. Sekikawa, S. Watanabe, T. Togashi, C. Chen, C. Zhang, Z. Xu, and J. Wang, "Generation of vacuum-ultraviolet light below 160 nm in a KBBF crystal by the fifth harmonic of a single-mode Ti:sapphire laser," J. Opt. Soc. Am. B **21**(2), 370 (2004).
25. C. T. Chen, G. L. Wang, X. Y. Wang, and Z. Y. Xu, "Deep-UV nonlinear optical crystal $KBe_2BO_3F_2$—discovery, growth, optical properties and applications," Appl. Phys. B **97**(1), 9–25 (2009).

26. T. Nakazato, I. Ito, Y. Kobayashi, X. Wang, C. Chen, and S. Watanabe, "149.8 nm, the shortest wavelength generated by phase matching in nonlinear crystals," in *Nonlinear Frequency Generation and Conversion: Materials and Devices XVI*, K. L. Vodopyanov and K. L. Schepler, eds. (SPIE, 2017).
27. M. Nisoli, S. D. Silvestri, and O. Svelto, "Generation of high energy 10 fs pulses by a new pulse compression technique," Appl. Phys. Lett. **68**(20), 2793–2795 (1996).
28. G. Fan, T. Balčiūnas, T. Kanai, T. Flöry, G. Andriukaitis, B. E. Schmidt, F. Légaré, and A. Baltuška, "Hollow-core-waveguide compression of multi-millijoule CEP-stable 3.2 μm pulses," Optica **3**(12), 1308 (2016).
29. J. M. Dudley and J. R. Taylor, "Ten years of nonlinear optics in photonic crystal fibre," Nat. Photonics **3**(2), 85–90 (2009).
30. D. E. Couch, D. D. Hickstein, D. G. Winters, S. J. Backus, M. S. Kirchner, S. R. Domingue, J. J. Ramirez, C. G. Durfee, M. M. Murnane, and H. C. Kapteyn, "Ultrafast 1 MHz vacuum-ultraviolet source via highly cascaded harmonic generation in negative-curvature hollow-core fibers," Optica **7**(7), 832 (2020).
31. J. C. Travers, T. F. Grigorova, C. Brahms, and F. Belli, "High-energy pulse self-compression and ultraviolet generation through soliton dynamics in hollow capillary fibres," Nat. Photonics **13**(8), 547–554 (2019).
32. J. C. Travers, W. Chang, J. Nold, N. Y. Joly, and P. St. J. Russell, "Ultrafast nonlinear optics in gas-filled hollow-core photonic crystal fibers [Invited]," J. Opt. Soc. Am. B **28**(12), A11 (2011).
33. F. Belli, A. Abdolvand, J. C. Travers, and P. S. J. Russell, "Highly efficient deep UV generation by four-wave mixing in gas-filled hollow-core photonic crystal fiber," Opt. Lett. **44**(22), 5509 (2019).
34. J. Nauta, A. Borodin, H. B. Ledwa, J. Stark, M. Schwarz, L. Schmöger, P. Micke, J. R. C. López-Urrutia, and T. Pfeifer, "Towards precision measurements on highly charged ions using a high harmonic generation frequency comb," Nucl. Instrum. Methods Phys. Res. Sect. B Beam Interact. Mater. At. **408**, 285–288 (2017).
35. A. Ozawa and Y. Kobayashi, "vuv frequency-comb spectroscopy of atomic xenon," Phys. Rev. A **87**(2), 022507 (2013).
36. C. Zhang, P. Li, J. Jiang, L. von der Wense, J. F. Doyle, M. E. Fermann, and J. Ye, "Tunable VUV frequency comb for ^{229m} Th nuclear spectroscopy," Opt. Lett. **47**(21), 5591 (2022).
37. C. Gohle, T. Udem, M. Herrmann, J. Rauschenberger, R. Holzwarth, H. A. Schuessler, F. Krausz, and T. W. Hänsch, "A frequency comb in the extreme ultraviolet," Nature **436**(7048), 234–237 (2005).
38. P. Rudawski, C. M. Heyl, F. Brizuela, J. Schwenke, A. Persson, E. Mansten, R. Rakowski, L. Rading, F. Campi, B. Kim, P. Johnsson, and A. L'Huillier, "A high-flux high-order harmonic source," Rev. Sci. Instrum. **84**(7), 073103 (2013).
39. G. Porat, C. M. Heyl, S. B. Schoun, C. Benko, N. Dörre, K. L. Corwin, and J. Ye, "Phase-matched extreme-ultraviolet frequency-comb generation," Nat. Photonics **12**(7), 387–391 (2018).
40. E. Appi, C. C. Papadopoulou, J. L. Mapa, C. Jusko, P. Mosel, A. Schönberg, J. Stock, T. Feigl, S. Ališauskas, T. Lang, C. M. Heyl, B. Manschwetus, M. Brachmanski, M. Braune, H. Lindenblatt, F. Trost, S. Meister, P. Schoch, A. Trabattoni, F. Calegari, R. Treusch, R. Moshammer, I. Hartl, U. Morgner, and M. Kovacev, "Synchronized beamline at FLASH2 based on high-order harmonic generation for two-color dynamics studies," Rev. Sci. Instrum. **92**(12), 123004 (2021).
41. A. Neumeier, M. Hofmann, L. Oberauer, W. Potzel, S. Schönert, T. Dandl, T. Heindl, A. Ulrich, and J. Wieser, "Attenuation of vacuum ultraviolet light in liquid argon," Eur. Phys. J. C **72**(10), (2012).
42. D. F. Swinehart, "The Beer-Lambert Law," J. Chem. Educ. **39**(7), 333 (1962).
43. Korth Kristalle GmbH, "Calcium flouride absorption data," (n.d.).
44. H. Fattahi, A. Alismail, H. Wang, J. Brons, O. Pronin, T. Buberl, L. Vámos, G. Arisholm, A. M. Azzeer, and F. Krausz, "High-power, 1-ps, all-Yb:YAG thin-disk regenerative amplifier," Opt. Lett. **41**(6), 1126 (2016).
45. S. Hädrich, J. Rothhardt, M. Krebs, S. Demmler, A. Klenke, A. Tünnermann, and J. Limpert, "Single-pass high harmonic generation at high repetition rate and photon flux," J. Phys. B At. Mol. Opt. Phys. **49**(17), 172002 (2016).
46. S. Salman, M. Fan, H. Tünnermann, P. Balla, J. Darvill, D. Laumer, V. Pecile, J. Fellinger, V. Shumakova, C. Mahnke, Y. Ma, C. Mohr, O. H. Heckl, C. M. Heyl, and I. Hartl, "Smart and agile 84 W fs Yb-fiber laser for spectroscopy," in *Conference on Lasers and Electro-Optics* (Optica Publishing Group, 2022), p. SF2M.1.
47. C. Zhang, S. B. Schoun, C. M. Heyl, G. Porat, M. B. Gaarde, and J. Ye, "Noncollinear Enhancement Cavity for Record-High Out-coupling Efficiency of an Extreme-UV Frequency Comb," Phys. Rev. Lett. **125**(9), (2020).